A chromodomain protein mediates heterochromatin-directed piRNA expression

Xinya Huang[a,1], Peng Cheng[a,1], Chenchun Weng[a], Zongxiu Xu[a], Chenming Zeng[a], Zheng Xu[a], Xiangyang Chen[a,2], Chengming Zhu[a,2], Shouhong Guang[a,b,2], and Xuezhu Feng[a,2]

[a]Ministry of Education Key Laboratory for Membraneless Organelles & Cellular Dynamics, Hefei National Laboratory for Physical Sciences at the Microscale, The First Affiliated Hospital of USTC, Division of Life Sciences and Medicine, University of Science and Technology of China, Hefei 230027, People's Republic of China; and [b]CAS Center for Excellence in Molecular Cell Science, Chinese Academy of Sciences, Hefei 230027, People's Republic of China

Edited by Victor R. Ambros, University of Massachusetts Medical School, Worcester, MA, and approved May 25, 2021 (received for review February 23, 2021)

PIWI-interacting RNAs (piRNAs) play significant roles in suppressing transposons, maintaining genome integrity, and defending against viral infections. How piRNA source loci are efficiently transcribed is poorly understood. Here, we show that in *Caenorhabditis elegans*, transcription of piRNA clusters depends on the chromatin microenvironment and a chromodomain-containing protein, UAD-2. piRNA clusters form distinct focus in germline nuclei. We conducted a forward genetic screening and identified UAD-2 that is required for piRNA focus formation. In the absence of histone 3 lysine 27 methylation or proper chromatin-remodeling status, UAD-2 is depleted from the piRNA focus. UAD-2 recruits the upstream sequence transcription complex (USTC), which binds the Ruby motif to piRNA promoters and promotes piRNA generation. Vice versa, the USTC complex is required for UAD-2 to associate with the piRNA focus. Thus, transcription of heterochromatic small RNA source loci relies on coordinated recruitment of both the readers of histone marks and the core transcriptional machinery to DNA.

piRNA | H3K27 | USTC | UAD-2 | chromatin remodeling

Eukaryotes utilize small RNA silencing pathways to repress transcription and ectopic recombination of transposable elements (TEs), and other repeats thus maintain genome integrity (1). In animal gonads, the PIWI-interacting RNAs (piRNAs) pathway is thought to recognize nascent transcripts of selfish genetic parasites such as TEs and guide the sequence specific silencing (2–4). The piRNA pathway relies on the cooperation between 22- to 30-nucleotide (nt)–long piRNAs and Piwi-clade Argonaute proteins to silence targets both at the cotranscriptional and posttranscriptional levels. The Piwi/piRNA pathway is essential for sex determination, defense against viruses, neoblast function, and germline fertility of diverse animal species (5–10). For example, MIWI (PIWIL1), MILI (PWIL2), and MIWI2 (PWIL4) are three Piwi proteins that are required for male fertility in mouse (11–13).

The piRNA biogenesis pathway is best understood in *Drosophila melanogaster*. Two major types of *Drosophila* piRNA clusters have been identified, the uni-strand and dual-strand clusters. Dual-strand piRNA clusters exhibit signatures of transcriptional silencing, for example, the heterochromatic mark histone H3 lysine 9 trimethylation (H3K9me3) (14, 15). The production of piRNAs from the dual-strand clusters requires the RDC complex composed of Rhino, Deadlock, and Cutoff. The RDC complex is anchored to H3K9me3-marked chromatin in part by Rhino's chromodomain. Rhino is a paralogue of heterochromatin protein-1 (HP1) and forms distinct foci in the nuclear periphery. Loss of Rhino induces a strong loss of piRNA production specifically from the dual-strand clusters (16, 17).

In *Caenorhabditis elegans*, mature piRNAs are predominantly 21 nt in length with a 5′ monophosphorylated uracil bias, known as 21U-RNAs (3, 18–20). Each piRNA is independently transcribed by RNA polymerase II (RNAP II) to generate 25- to 29-nt piRNA precursors with a conventional 5′ cap (21–23). Next, the precursors are exported out of the nucleus and bound by the PETISCO/PICS complexes, which might be involved in the 5′ end processing of piRNA precursors (24, 25). The conserved exonuclease PARN-1 is required for 3′ end trimming of piRNA precursors (26). The resulting mature piRNAs subsequently associate with the Piwi-type Argonaute protein PRG-1 and are 2′-O-methylated at the 3′ end by the *C. elegans* HEN1 ortholog HENN-1 enzyme (27, 28). Following target recognition by PRG-1, RNA-dependent RNA polymerases are recruited to elicit the generation of secondary small RNAs, also known as 22G-RNAs. The P-granule factors DEPS-1 and Mutator family proteins are also involved in efficient 22G-RNAs production (29, 30). The 22G-RNAs are then bound by a different set of worm-specific Argonaute proteins to silence gene expression transcriptionally and post-transcriptionally (3, 4, 31–33).

Two distinct classes of *C. elegans* piRNAs have been described. Type I piRNAs are encoded by two large transposon-rich genomic loci termed piRNA clusters on chromosome IV, which primarily contain intronic and intergenic piRNA transcription units enriched in Ruby motif (CTGTTTCA)–containing promoters (34, 35). Type II piRNAs are produced from annotated coding gene promoters across the *C. elegans* genome, which lack the Ruby motif and are unclustered. Both types of piRNA are transcribed as short piRNA precursors by RNAP II (21). Transcription of type I piRNAs relies

Significance

PIWI-interacting RNAs (piRNAs) are highly conserved among metazoan and act to distinguish self and nonself nucleic acids, silence transposable elements, defend against viral infections, protect germline integrity, and mediate transgenerational inheritance. How piRNA source loci are efficiently transcribed is poorly understood. In this work, we used both forward and reverse genetic approaches to decipher the molecular mechanisms of piRNA transcription in the *Caenorhabditis elegans* germline. We identified a chromodomain protein, UAD-2, that is required for piRNA focus formation, the association of an upstream sequence transcription complex with the piRNA genes, and piRNA production. This work suggested that transcription of heterochromatic piRNA loci relies on coordinated recruitment of both the readers of histone marks and the core transcriptional machinery.

Author contributions: X.H., P.C., X.C., C. Zhu, S.G., and X.F. designed research; X.H. and P.C. performed research; X.H., P.C., C.W., Zheng Xu, X.C., and C. Zhu contributed new reagents/analytic tools; X.H., P.C., C.W., Zongxiu Xu, and C. Zeng analyzed data; and X.H., P.C., X.C., C. Zhu, S.G., and X.F. wrote the paper.

The authors declare no competing interest.

This article is a PNAS Direct Submission.

[1]X.H. and P.C. contributed equally to this work.

[2]To whom correspondence may be addressed. Email: xychen91@ustc.edu.cn, zcm916@ustc.edu.cn, sguang@ustc.edu.cn, or fengxz@ustc.edu.cn.

This article contains supporting information online at https://www.pnas.org/lookup/suppl/doi:10.1073/pnas.2103723118/-/DCSupplemental.

Published June 29, 2021.

on the upstream sequence transcription complex (USTC), composed of PRDE-1, TOFU-5, TOFU-4, and SNPC-4, binding to the Ruby motif to promote autonomous expression of type I piRNA genes (36). Type II piRNAs are presumably regulated by the transcriptional machinery at the promoters from which they arise (18). In *Drosophila*, piRNA clusters generally reside within heterochromatin or in its close proximity. Most of their sequences correspond to transposon fragments or other repeats (37). Within the two piRNA clusters in *C. elegans*, most type I piRNA loci overlap with the facultative heterochromatin mark histone H3 lysine 27 trimethylation (H3K27me3) (38). How piRNAs are transcribed from the transcriptional silencing loci remains unknown.

Here, we used the USTC complex as a tool to search for factors required for piRNA production. We conducted a forward genetic screening and identified a chromodomain-containing protein, UAD-2. This screening yielded a point-mutation of UAD-2 that induced the depletion of USTC complex from the piRNA focus. UAD-2 is a potential reader of H3K27me3, recruits the USTC complex to piRNA promoters, and is required for piRNA biogenesis. Vice versa, the USTC complex is required for UAD-2 to associate with the piRNA focus. We designed a candidate-based RNA interference (RNAi) screening with TOFU-5::GFP transgene and found that the Polycomb repressive complex 2 (PRC2) and two chromatin-remodeling proteins, ISW-1 and MRG-1, are required for piRNA biogenesis as well. In the absence of H3K27me3 or under improper chromatin-remodeling status, the USTC complex and UAD-2 are depleted from the piRNA focus, and piRNAs dramatically decreased. Therefore, our data suggest that the transcription of heterochromatic small RNA source loci in *C. elegans* relies on the coordinated recruitment of both the readers of histone marks and the core transcriptional machinery to the genome.

Results

Forward Genetic Screening Identified UAD-2 That Is Required for piRNA Focus Formation and piRNA Production. We previously reported a USTC complex consisting of PRDE-1, SNPC-4, TOFU-4, and TOFU-5 that binds to piRNA promoters and directs piRNA transcription in *C. elegans* (36). USTC complexes form distinct piRNA foci in the germline nuclei, forming two spots in each mitotic nucleus and a single spot in the meiotic nucleus. LMN-1 is an ortholog of human lamin A/C and localizes to the inner side of the nuclear membrane (39). The piRNA focus also localizes to the inner nuclear membrane, as shown by the colocalization between TOFU-5::GFP and LMN-1::mCherry proteins (*SI Appendix*, Fig. S1*A*).

To understand the mechanism and regulation of piRNA transcription, we performed a forward genetic screening to search for factors that were required for piRNA focus formation. We chemically mutagenized TOFU-5::GFP animals and searched for mutants in which the piRNA foci were either disorganized or depleted by clonal screening (Fig. 1*A*). We isolated two USTC association-dependent mutants, termed *uad*, from 2,000 haploid genomes. One *uad-2*(*ust199*) allele was isolated from this screening in which the piRNA foci disappeared (Fig. 1*B*). We deep-sequenced the *uad-2*(*ust199*) genome and identified K06A5.1, an open reading frame that contained a C-to-T mutation and changed the amino acid arginine to a stop codon (Fig. 1*C*).

To further confirm that *k06a5.1* is *uad-2*, we generated two additional deletion alleles of *k06a5.1* by CRISPR/Cas9 mutagenesis with two single-guide RNAs (sgRNAs) and examined piRNA focus formation. The *uad-2*(*ust200*) allele deleted 618 nt of the genome sequence and caused a frame shift. The *uad-2*(*ust202*) allele removed nearly the entire protein coding region of the gene. The piRNA foci were depleted in both *uad-2*(*ust200*) and *uad-2*(*ust202*) mutants (Fig. 1*B*), yet the protein levels of TOFU-5 were unaffected in the three *uad-2* alleles (*SI Appendix*, Fig. S1*B*). An ectopically expressed UAD-2::mCherry transgene rescued piRNA focus formation in the germline nuclei in *uad-2*(*ust199*) mutants (*SI Appendix*, Fig. S1*C*). Therefore, *k06a5.1* is *uad-2*.

To investigate whether *uad-2* was required for the production of piRNAs, we isolated total small RNAs and deep-sequenced small RNAs 17 to 35 nt in size from *uad-2*(*ust199*), *uad-2*(*ust200*), and *uad-2*(*ust202*) mutants. piRNAs were dramatically depleted in the *uad-2* mutants compared to wild-type worms (Fig. 1*D* and *SI Appendix*, Fig. S1*D*). In *C. elegans*, piRNAs are 21 nt in length and start with 5′ U; therefore, piRNAs are also called 21U-RNAs (3, 40). Two types of piRNAs have been described in *C. elegans*. Type I piRNAs are predominantly transcribed from two broad regions on chromosome IV and contain an 8-nt upstream Ruby motif (CTGTTTCA) and a small YRNT motif, in which the T corresponds to the first U of the piRNA. Type II piRNAs are present outside of chromosome IV and lack the Ruby motif (20, 34). We assayed type I and II piRNAs and found that both classes of piRNAs were significantly depleted (Fig. 1*E*). Therefore, we concluded that *uad-2* was required for piRNA production.

To further study the function of UAD-2 in piRNA biogenesis, we constructed GFP-3xFLAG–tagged UAD-2 transgenes (abbreviated as UAD-2::GFP) using CRISPR/Cas9 directed in situ gene editing technology. Similar to the USTC complex, UAD-2::GFP exhibited distinct foci in the germline nuclei, with two spots in each mitotic nucleus and a single spot in the meiotic nucleus (Fig. 1*F* and *SI Appendix*, Fig. S2*A*). In the embryos, UAD-2 appeared to associate with chromatin and cosegregated with chromosomes during cell division (*SI Appendix*, Fig. S2*B*), suggesting that UAD-2 is a chromatin-binding protein. *uad-2* mutants exhibited a temperature-sensitive fertility defect. The brood size of *uad-2* animals was significantly decreased at 25 °C compared to 20 °C (*SI Appendix*, Fig. S2*C*).

Mutual Dependency of UAD-2 and the USTC Complex for Their Localization at the piRNA Focus in Germline Cells. Since UAD-2 is required for piRNA focus formation and piRNA production, we tested whether UAD-2 was essential for the USTC complex to associate with the piRNA promoters. We investigated the subcellular localization of other components of the USTC complex, including PRDE-1, TOFU-4, and SNPC-4, in *uad-2* mutants. Similar to GFP::TOFU-5, all three proteins failed to form piRNA foci in the germline of *uad-2* animals (Fig. 2*A*). In addition, chromatin immunoprecipitation (ChIP) of the USTC complex followed by deep sequencing (ChIP-seq) indicated that TOFU-5 failed to associate with piRNA genes in *uad-2* mutants (Fig. 2*B*).

Because UAD-2 and the USTC complex form a similar focus in the germline, two spots in each mitotic nucleus and a single spot in the meiotic nucleus, we tested whether they colocalized with each other. As expected, UAD-2 colocalized with PRDE-1 (Fig. 2*C*), suggesting that UAD-2 and the USTC complex localize to the same piRNA foci in each nucleus. Interestingly, we found that the USTC complex was also required for UAD-2 localization. In *prde-1* and *tofu-4* mutants, UAD-2 failed to accumulate at the piRNA foci (Fig. 2*D*), suggesting a mutual dependency of UAD-2 and the USTC complex for proper subcellular localization. Noticeably, in our previous work, we conducted extensive yeast-two-hybrid and immunoprecipitation mass spectrometry (IP-MS) experiments with PRDE-1, SNPC-4, TOFU-4, and TOFU-5 but failed to identify UAD-2 in any of the experiments (36), suggesting that UAD-2 either does not directly interact with the USTC complex or that their protein–protein interaction is transient or very weak.

H3K27me3 Promotes piRNA Focus Formation and piRNA Production. UAD-2 contains a chromodomain and a serine/arginine (SR)-rich domain (Fig. 1*C*). Chromodomains are highly conserved protein structural domains and are one of the major readers of histone methylation marks in proteins or protein complexes that are capable to detect and bind methylated histones (41). SR-rich splicing factors contain an RNA-binding domain and an SR-rich

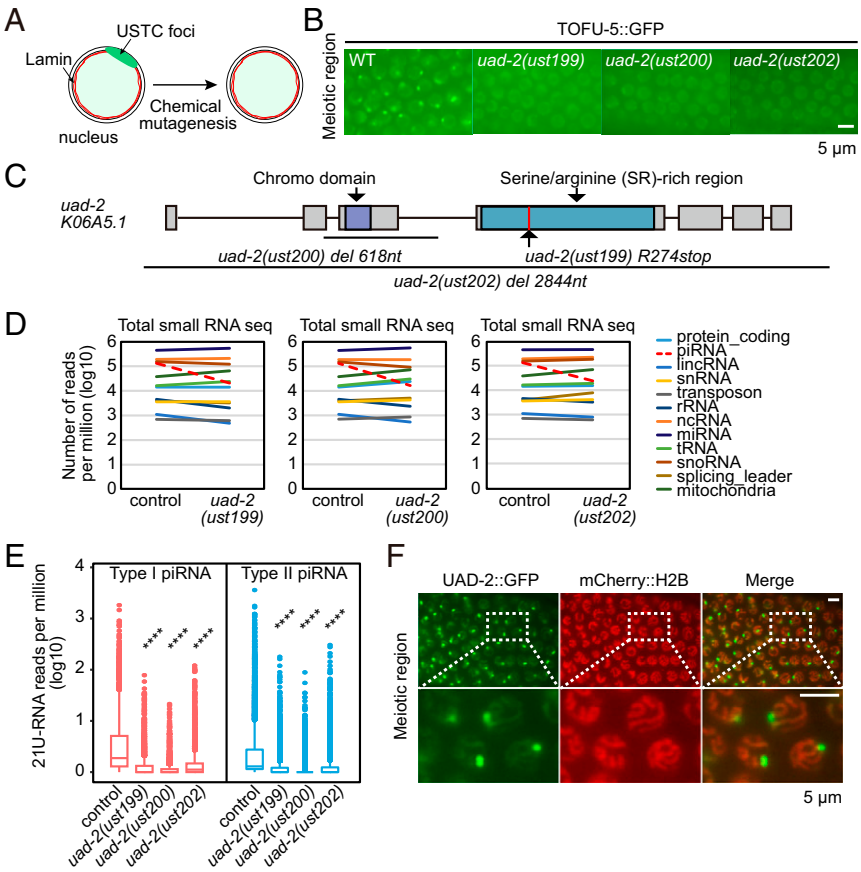

Fig. 1. UAD-2 encodes a chromodomain-containing protein required for piRNA production. (*A*) Schematic diagram of the forward genetic screening for abnormal piRNA focus formation in *C. elegans* germline nuclei. (*B*) Images of representative meiotic germline nuclei of the indicated young adult animals. (*C*) Schematic of *uad-2* exon and domain structure. The deletion alleles *ust200* and *ust202* were constructed by CRISPR/Cas9 technology. All three alleles were null alleles. (*D*) Deep sequencing of total small RNAs in the indicated animals. Red dashed line indicates piRNAs. (*E*) Boxplot showing the number of type I and type II piRNA reads per million of the indicated animals at the young adult stage. Significance was tested with the unpaired Wilcoxon test, ****$P < 2.2 \times e^{-16}$. (*F*) Images of representative meiotic germline nuclei in young adult animals. UAD-2::GFP (green) colocalized with the chromatin marker mCherry::H2B (red). (Scale bars, 5 μm.)

domain required for protein–protein interactions (42). SR proteins function both in basic splicing reactions and as components of splicing enhancer complexes. The protein structure suggests that UAD-2 may function in the recognition of histone methylation marks and/or the processing of RNA transcripts.

Chromodomains are of ∼40– to 50–amino acid residues that are commonly found in proteins associated with chromatin remodeling and manipulation (41). Chromodomain-containing proteins regulate gene transcription by identifying and binding to methylated lysine residues that exist on the surface of chromatin proteins. The *C. elegans* genome encodes 21 chromodomain-containing proteins, most of which have unknown functions (*SI Appendix*, Fig. S3*A*). One of these chromodomain proteins, CEC-4, was shown to recruit H3K9me3-marked heterochromatin to the inner nuclear membrane region (43). We tested whether other chromodomain proteins, besides UAD-2, were engaged in piRNA focus formation. Notably, knocking down *mrg-1* but not any of the other 19 chromodomain proteins inhibited piRNA focus formation in the germline (*SI Appendix*, Fig. S3*B*). MRG-1 is the ortholog of human MORF4L1 (mortality factor 4 like 1) and MORF4L2 (mortality factor 4 like 2). MRG-1 is broadly expressed and is necessary for chromatin to anchor to the inner membrane in differentiated cells; it also protects germ cells against conversion into other cell types (44).

A proper chromatin microenvironment was shown to be required for piRNA production in both *Drosophila* and *C. elegans* (38, 45). The piRNA clusters in *C. elegans* are enriched with H3K27me3 marks. To investigate how and why UAD-2 promotes piRNA generation, we conducted a candidate-based reverse genetic screening and searched for factors that were also required for piRNA focus formation. We selected 239 genes that are involved in chromatin modification and histone modification and knocked down these genes using exogenous RNAi in *C. elegans* (*SI Appendix*, Table S1). Then, we examined the TOFU-5::GFP foci using fluorescence microscopy. Among the 239 genes, we found that knocking down 12 genes, including *mes-2*, *mes-3*, *mes-4*, *mes-6*, *isw-1*, *mrg-1*, *sun-1*, *R151.8*, and *epc-1*, significantly inhibited piRNA focus formation (Fig. 3*A*).

MES-2, MES-3, and MES-6 are subunits of the PRC2 complex, which is engaged in H3K27me3 (46). MES-2 is a homolog of *Drosophila* E(Z) and human EZH2. It contains a SET domain and functions as a histone methyltransferase. MES-2 is the only known H3K27 methyltransferase encoded in the *C. elegans* genome (46). Knocking down PRC2 components depleted TOFU-5, SNPC-4, PRDE-1, and UAD-2 aggregation in the inner nuclear membrane without changing the protein levels of TOFU-5::GFP (Fig. 3*B* and *SI Appendix*, Fig. S4 *A* and *B*), suggesting that H3K27me3 was necessary for piRNA focus formation. This result is consistent with a previous report that the piRNA clusters were enriched with H3K27me3 modification (38). We conducted ChIP analysis of TOFU-5 and SNPC-4 and confirmed that *mes-2*, *mes-3*, and *mes-6* were required for TOFU-5 and SNPC-4 to bind piRNA clusters (Fig. 3*C* and *SI Appendix*, Fig. S4*C*).

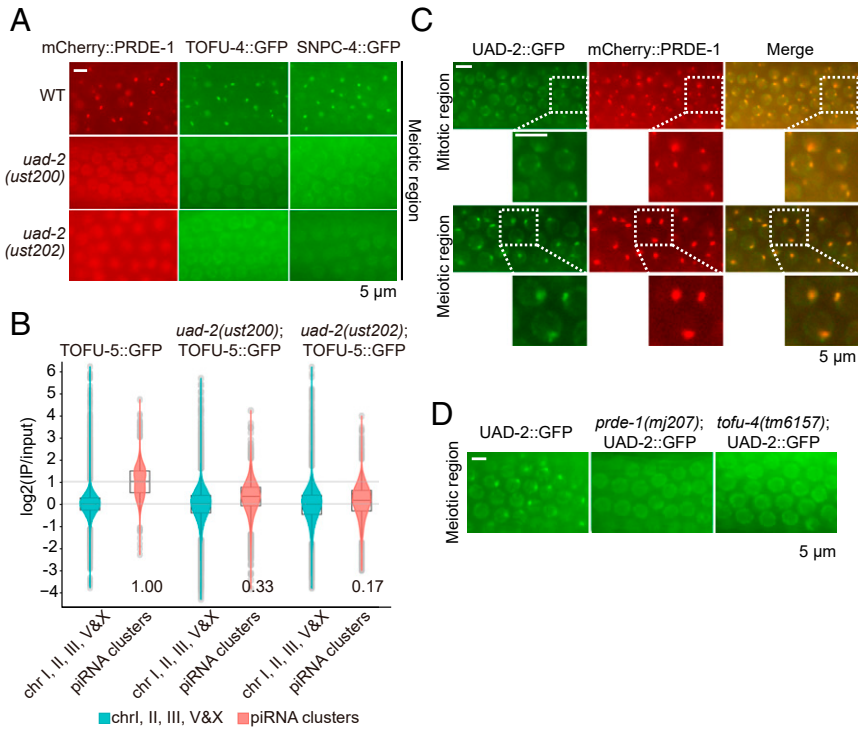

Fig. 2. UAD-2 is required for USTC complex association with piRNA genes. (*A*) Images of representative meiotic germline nuclei of the indicated young adult animals. (*B*) Quantification of ChIP-seq signals on chromosome IV and other chromosomes (I, II, III, V, and X). The piRNA clusters exist on chromosome IV. Signal was calculated in 1-kb bins. TOFU-5::GFP failed to be enriched at piRNA clusters in *uad-2*(*ust200*) and *uad-2*(*ust202*) animals. (*C*) Colocalization of UAD-2::GFP (green) with mCherry::PRDE-1 (red) in mitotic and meiotic germline nuclei in young adult animals. (*D*) Images of representative meiotic germline nuclei of the indicated young adult animals. UAD-2::GFP failed to form piRNA focus in *prde-1*(*mj207*) and *tofu-4*(*tm6157*) animals. (Scale bars, 5 μm.)

We then tested whether H3K9 methylation is required for piRNA focus formation. Heterochromatin is divided into two classes: H3K9me3-marked constitutive heterochromatin and H3K27me3-marked facultative heterochromatin. In *Drosophila*, deposition of H3K9me3 by dSETDB1, which can be subsequently bound by Rhino, is required for piRNA cluster transcription (45, 47). In *C. elegans*, H3K9 methylation is necessary to silence and anchor repeat-rich heterochromatin at the nuclear periphery (43, 45, 48). MET-2, a SETDB1 homolog, mediates mono- and dimethylation of H3K9. SET-25 is necessary for H3K9me3 modification. In *met-2*(-);*set-25*(-) double mutants, H3K9 modifications were depleted (48), yet the piRNA foci were maintained (Fig. 3*B*), suggesting that H3K9 methylation marks were not required for piRNA focus formation in *C. elegans*. Therefore, we concluded that the facultative heterochromatin mark H3K27me3 but not the constitutive heterochromatin mark H3K9me3 promotes UAD-2 and USTC focus assembly and inner nuclear membrane anchoring in *C. elegans*.

To confirm that *mes-2*, *mes-3*, and *mes-6* were required for piRNA production, we first utilized a piRNA sensor assay, in which the GFP-labeled sensor transgene is silenced in wild-type germlines but desilenced when piRNA production is compromised (24). The depletion of *snpc-4*, *tofu-5*, *mes-2*, *mes-3*, or *mes-6* by RNAi desilenced the piRNA sensor in the germline, which is consistent with their functions in piRNA expression (Fig. 3*D*). Next, we isolated total small RNAs from the mutants and deep-sequenced small RNAs ranging from 17 to 35 nt in length. Since homozygous *mes-2*, *mes-3*, and *mes-6* mutants are maternal sterile, the mutants were first collected from balanced strains and the small RNAs were isolated from their F1 progeny (*SI Appendix*, Fig. S5*A*). Both type I and II piRNAs were dramatically depleted in all these mutants (Fig. 3*E* and *SI Appendix*, Fig. S5 *B* and *C*), suggesting that proper H3K27me3 modification was essential for piRNA production. Noticeably, piRNAs guide H3K27 trimethylation at the targeted genomic sites via the nuclear RNAi pathway (33). Whether and how an H3K37m3 methylation-involved feedback loop coordinates piRNA production and activity requires further investigation.

Chromatin Microenvironment Promotes piRNA Focus Formation and piRNA Production. Chromatin-remodeling factors play important roles in shaping the structure and subnuclear position of chromatin as well as transcription regulation. The ISWI protein promotes chromatin remodeling by using energy from ATP hydrolysis to slide or reposition nucleosomes (49). In *C. elegans*, ISW-1 integrates organismal responses against nuclear and mitochondrial stress and affects longevity (50, 51). MRG-1 is a chromodomain protein and likely recognizes germline-expressed genes using the epigenetic mark H3K36me, which is generated by MES-4. MRG-1 is required to silence repetitive genes and maintain genome integrity (44). Both ISW-1 and MRG-1 were required for piRNA focus formation at the inner nuclear membrane (Fig. 4*A* and *SI Appendix*, Fig. S6*A*). We confirmed that ISW-1 was required for TOFU-4, TOFU-5, and SNPC-4 to associate with piRNA genes by ChIP analysis (Fig. 4 *B* and *C* and *SI Appendix*, Fig. S6 *B* and *C*). Using the piRNA sensor, we found that ISW-1 and MRG-1 were required for the silencing of the piRNA sensor (Fig. 4*D*). We then deep-sequenced small RNAs from *isw-1* and *mrg-1* mutant animals and found that piRNAs significantly decreased in the mutants (Fig. 4*E* and *SI Appendix*, Fig. S7 *A*–*D*). Both type I and II piRNAs were depleted (*SI Appendix*, Fig. S7*E*). These data suggested that chromatin-remodeling factors play important roles in recruiting UAD-2 and USTC components to piRNA clusters and driving piRNA production.

ISW-1 is a component of the ISWI/NURF complex, which also includes NURF-1, PYP-1, and RBA-1 (*SI Appendix*, Fig. S8*A*). MRG-1 belongs to a SWR1/SRCAP complex, containing six other proteins (*SI Appendix*, Fig. S8*B*). We tested whether both complexes

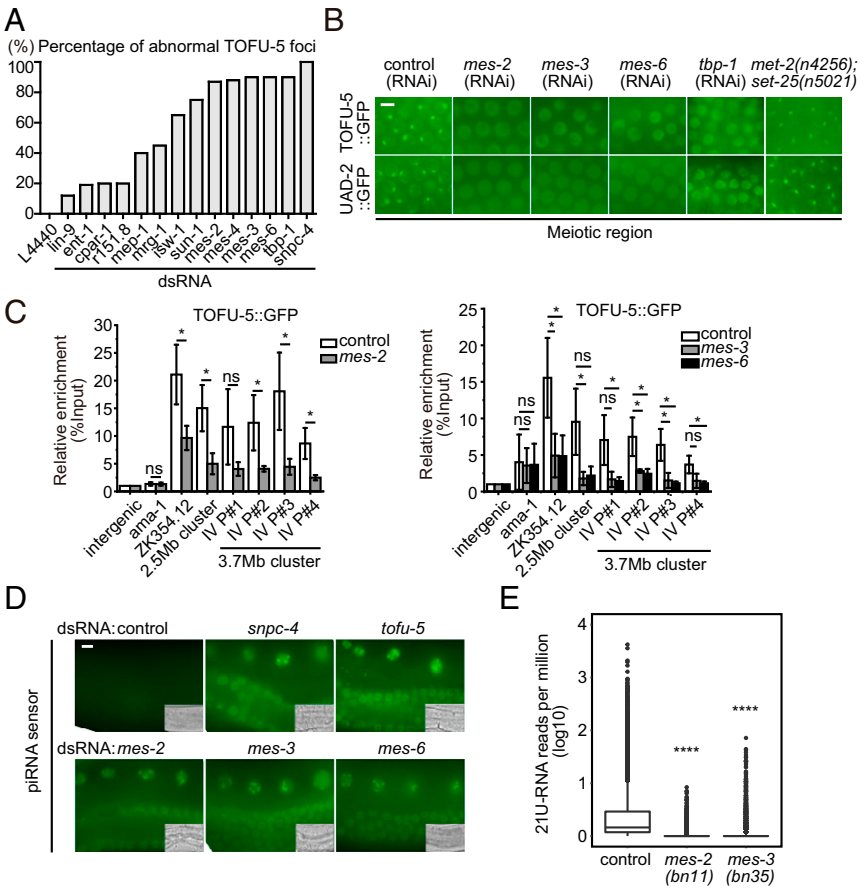

Fig. 3. PRC2 is required for piRNA production. (*A*) A candidate-based RNAi screening identified genes required for piRNA focus formation. $n > 50$ animals (*SI Appendix*, Table S1). (*B*) Images of representative meiotic germline nuclei of the indicated young adult animals. TOFU-5::GFP and UAD-2::GFP failed to form piRNA focus in *mes-2*, *mes-3*, or *mes-6* knockdown animals. TBP-1 encodes the *C. elegans* ortholog of human TBP, which is essential for transcriptional regulation. MET-2 and SET-25 perform H3K9 methylation. (*C*) Relative enrichment of TOFU-5 by ChIP assay in animals treated with the indicated dsRNAs. Mean ± SD, $n = 3$. *$P < 0.05$, ns, not significant. (*D*) Representative bright field and fluorescence microscopy images of piRNA sensor expression in indicated animals. Depletion of *mes-2*, *mes-3*, or *mes-6* by RNAi desilenced the piRNA sensor in the germline. (*E*) Boxplot showing the normalized number of piRNA reads per million in the indicated animals at the young adult stage. *mes-2*(*bn11*) and *mes-3*(*bn35*) homozygous mutants were maternal sterile and were isolated from balancers. Significance was tested with the unpaired Wilcoxon test, ****$P < 2.2 \times e^{-16}$. (Scale bars, 5 μm.)

were required for piRNA focus formation. Strikingly, only ISW-1 and MRG-1 but not other factors within the two complexes were essential for piRNA focus formation (Fig. 4 *F* and *G* and *SI Appendix*, Fig. S8 *C* and *D*). The effectiveness of RNAi was confirmed by counting the brood size of feeding RNAi-treated animals (*SI Appendix*, Fig. S8*E*). We conclude that ISW-1 and MRG-1 may use alternative mechanisms to promote piRNA focus formation and transcription.

Elevated Temperature Suppresses piRNA Production by Depleting the piRNA Foci-Localized UAD-2 and the USTC Complex. piRNAs play important roles in the response of animals to environmental alterations, memorize the stimuli, and help progenies adapt to environmental changes (40). When nematodes were grown at 25 °C, which is a higher temperature than normal laboratory culturing conditions, the expression of piRNAs decreased (31, 52). We found that both the USTC complex and UAD-2 failed to aggregate at piRNA foci when animals were grown at 25 °C (Fig. 5*A*). ChIP assays further revealed that TOFU-4 failed to bind to piRNA genes at higher temperatures (Fig. 5 *B* and *C*). At 25 °C, the amounts of total piRNAs and type I and II piRNAs were all reduced (Fig. 5 *D* and *E*). These data suggested that environmental stimuli may modulate piRNA expression by altering the association of UAD-2 and the USTC complex with piRNA genes to regulate piRNA transcription.

UAD-2 Binds H3K27me3 In Vitro. To test whether UAD-2 directly binds to histone proteins, we set up an in vitro peptide pull-down assay (Fig. 6*A*). We first expressed MBP-fused UAD-2 proteins in bacteria and purified by amylose resin. Then the proteins were incubated with biotin-labeled histone H3 peptides followed by precipitation with streptavidin agarose beads. The pelleted proteins were then resolved on an sodium dodecyl sulfate polyacrylamide gel electrophoresis (SDS-PAGE) and stained by Coomassie blue. Since UAD-2 encodes a large internal disordered region, we failed to express the recombinant MBP-tagged full-length UAD-2 (MBP-UAD-2 full-length) (*SI Appendix*, Fig. S9*A*). Therefore, we expressed and purified MBP-tagged UAD-2 chromodomain (amino acids 57 to 124) (Fig. 6*B*). As a control, we expressed and purified MBP-tagged CEC-4 CD domain (amino acids 25 to 141), which has been shown to bind H3K9me3 peptide (43). Consistent with previous results, CEC-4 binds to H3K9me3 peptide (Fig. 6*C* and *SI Appendix*, Fig. S9 *B*, *Right*) but not H3K9 peptide (Fig. 6*C* and *SI Appendix*, Fig. S9 *B*, *Left*). UAD-2 does not bind either H3K9 or H3K9me3 peptides. Interestingly, UAD-2 binds to H3K27me3 peptide (Fig. 6*D* and *SI Appendix*, Fig. S9 *C*, *Right*) but not H3K27 peptide (Fig. 6*D* and *SI Appendix*, Fig. S9 *C*, *Left*). CEC-4 does not bind to either of these two peptides. Therefore, we conclude that UAD-2 may directly associate with H3K27me3.

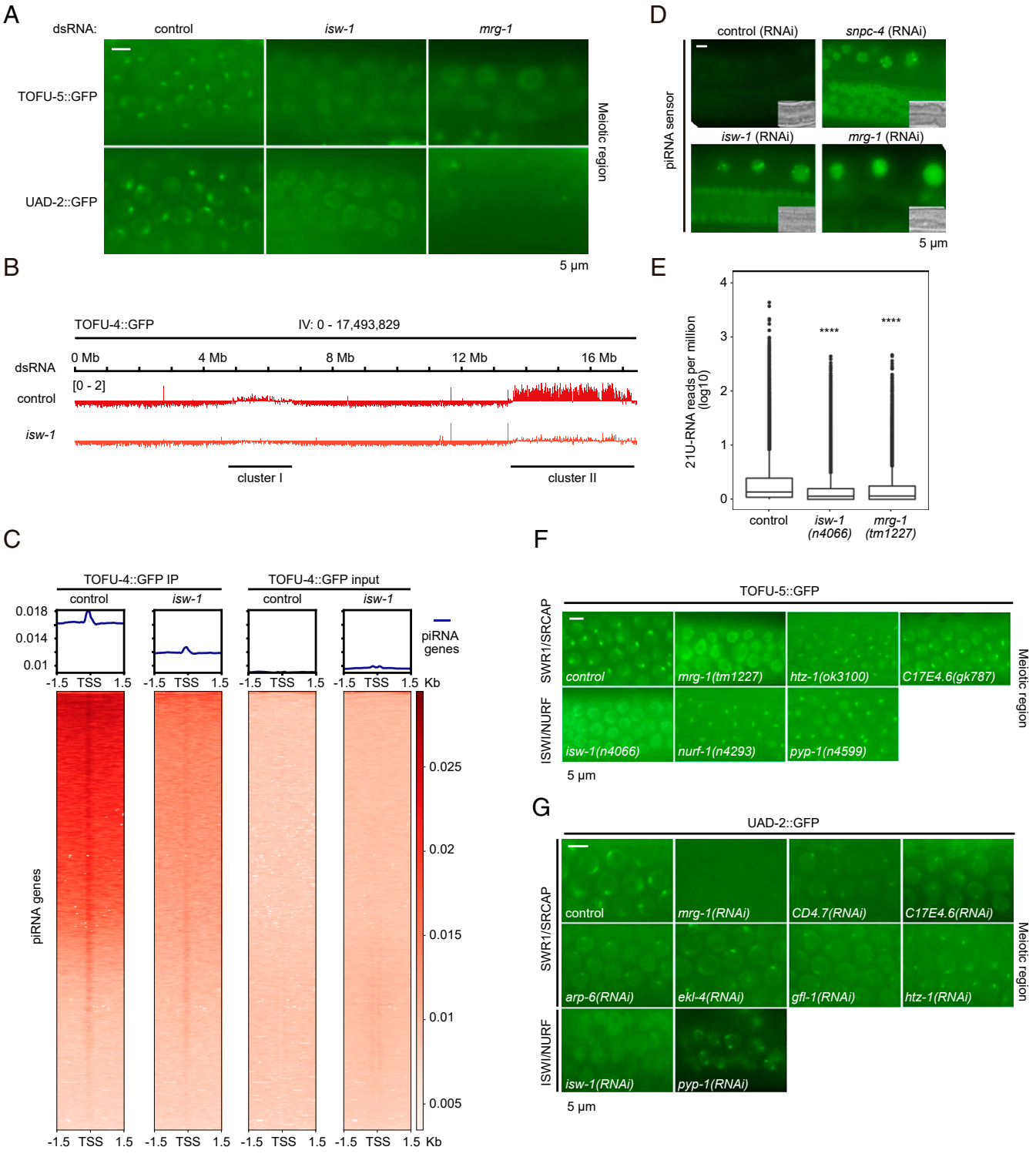

Fig. 4. Chromatin-remodeling factors ISW-1 and MRG-1 are required for piRNA production. (*A*) Images of representative meiotic germline nuclei of the indicated young adult animals. Depletion of *isw-1* and *mrg-1* by RNAi suppressed piRNA focus formation. (*B*) ChIP-seq revealed the binding profiles of TOFU-4::GFP across chromosome IV in the indicated animals at the young adult stage. ChIP-seq signals were normalized by MACS2 and log2-transformed. (*C*) Heat map of ChIP-seq binding profiles of TOFU-4::GFP around all piRNA transcription start sites (TSSs). (*D*) Representative bright field and fluorescence microscopy images of piRNA sensor expression in indicated animals. Depletion of *isw-1* or *mrg-1* by RNAi desilenced the piRNA sensor in the germline. (*E*) Boxplot showing the number of normalized piRNA reads per million in the indicated animals at the young adult stage. Reads were normalized to total RNA reads. *isw-1*(*n4066*) and *mrg-1*(*tm1227*) homozygous mutants were sterile and were isolated from balancers. Significance was tested with unpaired Wilcoxon test, $****P < 2.2 \times e^{-16}$. (*F*) Images of representative meiotic germline nuclei of the indicated young adult animals. TOFU-5::GFP failed to form piRNA focus in *isw-1*(*n4066*) and *mrg-1*(*tm1227*) mutants but not in other mutants of ISWI/NURF and SWR1/SRCAP complexes. (*G*) Images of representative meiotic germline nuclei of the indicated young adult animals. Depletion of *isw-1* and *mrg-1* but not other components of ISWI/NURF and SWR1/SRCAP complexes by RNAi suppressed UAD-2::GFP focus formation.

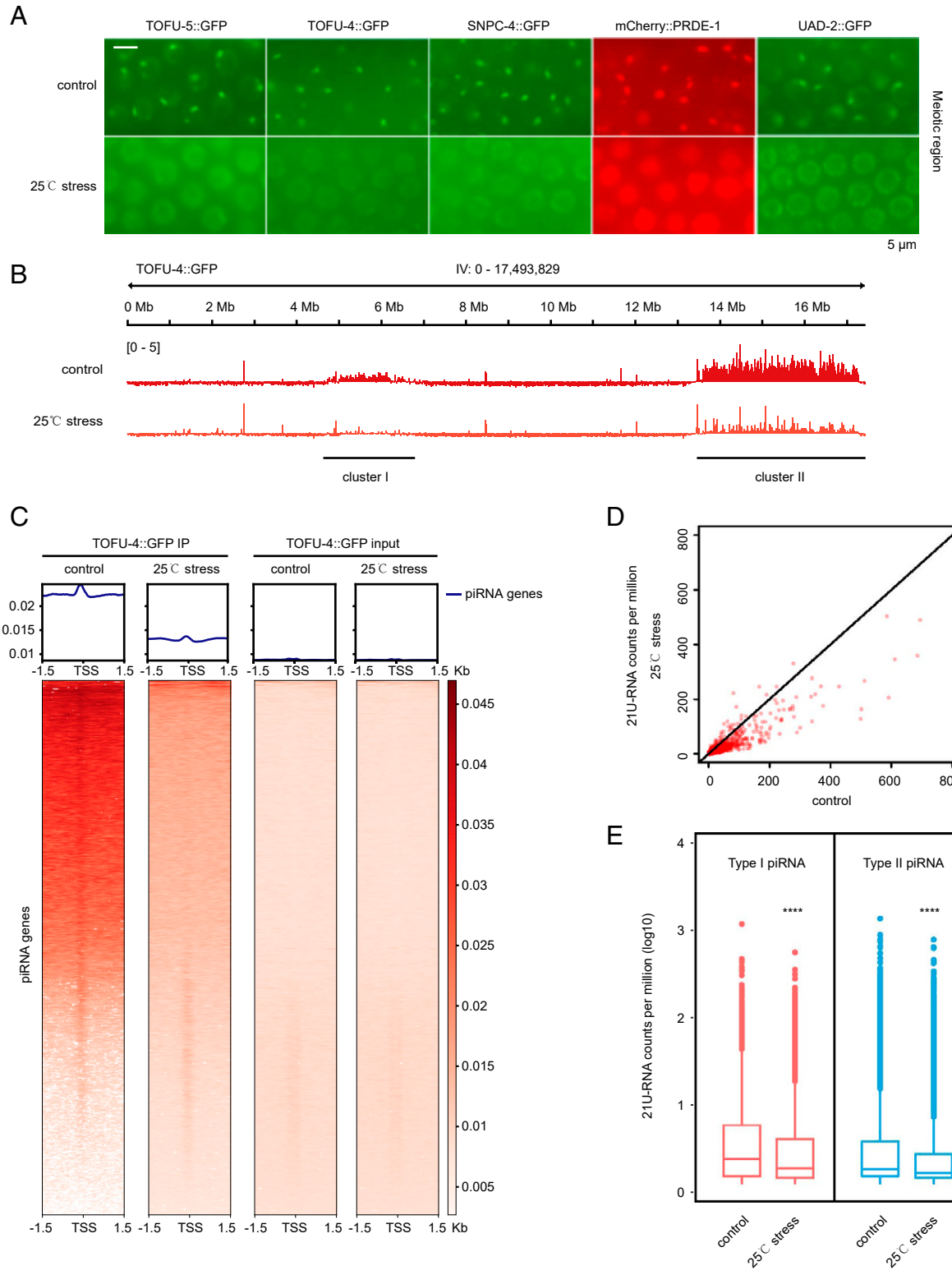

Fig. 5. High temperature suppresses piRNA focus formation and reduces piRNA expression. (*A*) Images of representative meiotic germline nuclei of the indicated young adult animals. The USTC complex and UAD-2::GFP failed to form piRNA foci after animals were grown at 25 °C for two generations. (*B*) ChIP-seq assay revealed the binding profile of TOFU-4::GFP across chromosome IV in the indicated animals at the young adult stage. ChIP signals were normalized by MACS2 and log2 transformed. (*C*) Heat map of ChIP-seq binding profiles of TOFU-4::GFP around all piRNA TSSs at 20 °C and 25 °C, respectively. (*D*) Scatterplots comparing the numbers of piRNA reads between animals growing at different temperatures. (*E*) Boxplot showing the numbers of type I and type II piRNA reads per million in the indicated animals at the young adult stage. Reads were normalized to total RNA reads. Significance was tested with unpaired Wilcoxon test, $****P < 2.2 \times e^{-16}$.

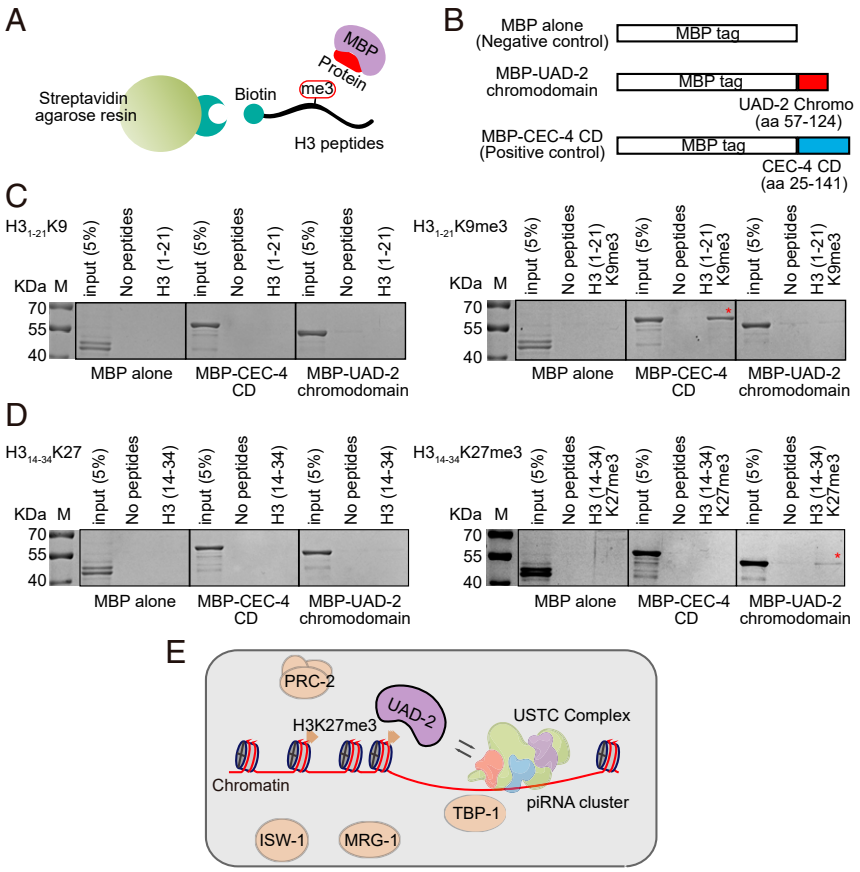

Fig. 6. UAD-2 chromodomain binds H3K27me3 peptide in vitro. (*A*) Schematic of the histone peptide pull-down assay. (*B*) Schematic diagram of the MBP-tagged UAD-2 chromodomain and CEC-4 CD domain. (*C* and *D*) Coomassie blue–stained SDS-PAGE gels showing binding of the indicated proteins to biotinylated-labled histone H3 peptides. MBP alone served as negative control. (*C*) $H3_{1–21}$K9 (*Left*) and $H3_{1–21}$K9me3 (*Right*), (*D*) $H3_{14–34}$K27 (*Left*), and $H3_{14–34}$K27me3 (*Right*). (*E*) A working model of UAD-2–directed piRNA expression. The PRC2 complex methylates H3K27, which is recognized by the chromodomain-containing protein UAD-2. ISW-1 and MRG-1 aid in maintaining a proper chromatin microenvironment. UAD-2 further facilitates the deposition of the USTC complex at piRNA genes and subsequently promotes piRNA transcription. TBP-1 encodes the *C. elegans* ortholog of human TBP, which is essential for transcriptional regulation.

Discussion

Taken together, these data suggest that UAD-2 promotes the biogenesis of piRNAs by binding to piRNA clusters and subsequently facilitating the deposition of the USTC to the genome (Fig. 6*E*). H3K27me3 methyltransferase and chromatin-remodeling factors could modulate piRNA production through the deposition of UAD-2 and USTC complexes. Additionally, the environmental stimuli may modulate piRNA expression by altering the association of UAD-2 and the USTC complex with piRNA genes as well. UAD-2 contains a chromodomain, which likely recognizes modified histone tails. Whether and how UAD-2 directly recognizes H3K27me3 and recruits the USTC complex requires further investigation.

The Functions of UAD-2. Small RNA source loci embedded in heterochromatin and transcribed are a hallmark of genome defense pathways in a variety of organisms. In plants, SHH1, a reader of H3K9me marks, recruits the RNA polymerase IV to heterochromatin to transcribe small RNA precursors. In *Drosophila*, Rhino recognizes H3K9me3 marks, together with its cofactors Deadlock and Cutoff, and promotes piRNA transcription from the repressive heterochromatin (45). Rhino's chromodomain binds mono, di-, or trimethylated H3K9 to anchor Deadlock and Cutoff to dual-strand piRNA clusters in ovarian germline cells and therefore licenses dual-strand transcription of piRNA source loci (17).

We have not identified a homolog of UAD-2 in other nonnematode species. UAD-2 forms distinct piRNA focus that localizes to the inner nuclear membrane in *C. elegans* germline cells. We suspect that UAD-2, as a chromodomain protein, functions in piRNA transcription and recognition of the heterochromatic mark H3K27me3. *Dom-3* in *C. elegans* is the ortholog of *Cutoff*. It will be interesting to test whether UAD-2/DOM-3 uses the similar mechanism of Rhino–Deadlock–Cutoff to coordinate heterochromatin status and transcriptional machinery to mediate piRNA expression.

In *C. elegans* embryos, a chromodomain factor CEC-4 binds preferentially H3K9 trimethylation and localizes at the nuclear envelope. CEC-4 is required for endogenous heterochromatin anchoring (43). In differentiated tissues, MRG-1 plays a central role of the heterochromatin-sequestering pathway as well. MRG-1 is the homolog of chromodomain protein MRG15 in humans and promotes the perinuclear anchoring of heterochromatin independently of CEC-4 and H3K9 methylation in intestinal cells (44). Here, we showed that MRG-1 is also required for H3K27me3-related heterochromatin sequestering and piRNA expression, suggesting a more broad function of MRG-1.

The *C. elegans* genome encodes 21 chromodomain proteins, most of which have unknown functions (*SI Appendix*, Fig. S3*A*). The two chromodomain proteins UAD-2 and MRG-1 are required for piRNA focus formation and piRNA biogenesis. Yet knocking down of the other 19 chromodomain proteins have no

obvious impact on piRNA focus formation in the germline (*SI Appendix*, Fig. S3*B*). It will be very interesting to investigate the subnuclear localization and functions of other 19 chromodomain proteins.

UAD-2 and the USTC Complex. *uad-2* activity is required for USTC focus formation (Figs. 1*B* and 2*A*). Vice versa, the USTC complex is required for UAD-2 to enrich at the piRNA focus (Fig. 2*D*). Our previous work has conducted extensive yeast-two-hybrid and IP-MS experiments with PRDE-1, SNPC-4, TOFU-4, and TOFU-5 but failed to identify UAD-2 in any of the experiments, suggesting that UAD-2 either does not directly interact with the USTC complex or that their protein–protein interaction is transient or very weak.

UAD-2 encodes a chromodomain in the N terminus and an unknown domain in C terminus. In *Drosophila*, Rhino harbors a chromodomain in the N terminus and a chromo-shadow domain in the C terminus. Rhino binds the N terminus of Deadlock protein through a novel interface formed by the beta-sheet in the Rhino's chromoshadow domain (53). Further identification of the proteins directly interact with UAD-2 will shed light on the specific mechanisms underlying piRNAs transcription in *C. elegans*.

UAD-2 contains an SR-rich domain, which is widely found in SR proteins. SR proteins are RNA-binding proteins known as constitutive and alternative splicing regulators. Diverse SR proteins play partially overlapping but distinct roles in transcription-coupled splicing and messenger RNA (mRNA) processing in the nucleus. Shuttling SR proteins act as adaptors for mRNA export and as regulators for translation in the cytoplasm. piRNA precursors are transcribed by RNAP II as individual transcripts followed by a number of processing steps and exported to cytoplasm for final maturation. UAD-2 may use its SR domain to participate in diverse protein–protein and protein–RNA interactions.

Chromatin Environment in piRNA Transcription. Recent work reported that clustered and dispersed piRNA loci have distinct chromatin environments in *C. elegans*. Type I piRNAs are predominantly transcribed from regulated domains enriched in H3K27me3 (38), and type II piRNAs are derived from the promoters of coding genes throughout the genome (20). Both classes of piRNAs are depleted in *tofu-4*, *tofu-5*, and *snpc-4* mutants, and only type I piRNAs are decreased in *prde-1* mutants (23, 36, 54). Our results showed that UAD-2 and H3K27me3 modification are required for all types of piRNA production (Fig. 1*E* and *SI Appendix*, Fig. S5*C*). While all components of USTC complex bind type I piRNA promoters, PRDE-1 and TOFU-4 exhibit less affinity to type II piRNA promoters. It is unclear how UAD-2 and local chromatin environment affect the USTC binding to different types of piRNA promoters. In *Drosophila*, the Rhino–Deadlock–Cutoff complex licenses transcription of dual-stranded piRNA clusters by preventing RNAP II termination (17). Whether and how UAD-2 and USTC complex cooperate with the H3K27me3 marks to promote RNAP II pausing in *C. elegans* during type I and type II piRNA transcription require further investigation. Our genetic and in vitro peptide pull-down experiments have shown that UAD-2 chromodomain could bind H3K27me3. However, we have not exhaustively excluded the possibility that UAD-2 may associate with other type of histone modification marks.

The result that *mes-4* is required for piRNA production is intriguing. In *C. elegans*, H3K36 methylation is carried out by two histone methyltransferases, MES-4 and MET-1. MES-4 is the homolog of mouse NSD1 and methylates H3K36me2/3 in a transcription-independent manner and functions in both the germline and early embryos (55, 56). MET-1, the homolog of *Saccharomyces cerevisiae* Set2, generates H3K36me3 in embryos (57, 58). We found that *mes-4* but not *met-1* is required for piRNA focus formation (Fig. 3*A*). Knocking down *mes-4* by RNAi derepressed a GFP-based small interference RNA (siRNA) sensor, 22G siR-1, suggesting that MES-4 is involved in siRNA production or activity (28). The exact molecular function of MES-4 in piRNA expression is unknown. H3K27me3 and H3K36me3 marks occupy mutually exclusive domains on the autosomes in *C. elegans* (59–61). Loss of MES-4 induces the spreading of H3K27me3 to germline genes, thereby reducing the level of H3K27me3 both on the autosomes and the X chromosomes (61). It is likely that the presence of MES-4 and H3K36me marks promotes the accumulation of H3K27me3 on the genome of piRNA clusters. Further investigation of the roles of MES-4 and H3K36me3 marks in piRNA transcription are required to understand the regulation of UAD-2 and USTC complex in piRNA expression. Similarly, the chromatin-remodeling proteins MRG-1 and ISW-1 are required for piRNA focus formation and piRNA biogenesis. MRG-1 is required for the repression of genes that are mis-regulated in *mes-4* mutants (44, 56, 62). ISW-1 is the homolog of *S. cerevisiae* Isw1. In *yeast*, Isw1 associates with H3K36me3 nucleosomes, delays the release of initiated RNAP II into elongation phase, and facilitates chromatin modifications (63, 64). Whether MRG-1, ISW-1, and MES-4 act cooperatively to promote the activity of PRC2 complex on genome of piRNA clusters requires further investigation.

SNPC-4 and TOFU-5, components of the USTC complex, contain SANT domains (65). Similarly, the chromatin-remodeling protein ISW-1 contains two SANT domains. They are both required for piRNA production. Previous studies have shown that SANT domains couple histone tail binding to enzymatic activity and are important for nucleosome sliding activity, which has been reported to be involved in nucleosome spacing in both yeast and mammals (66). The *C. elegans* genome encodes 18 SANT domain-containing proteins. We knocked down these genes by exogenous RNAi and found that R151.8, as a previously uncharacterized protein, is required for piRNA focus formation (Fig. 3*A*). However, the function of R151.8 and whether the presence of its SANT domain is required for piRNA production are still unclear.

Using the subcellular localization of UAD-2 and the USTC complex as reporters, we have searched for factors that are engaged in H3K27me3-marked facultative heterochromatin compaction and subnuclear localization. SUN-1 is an inner nuclear membrane adaptor protein and is essential for centrosome localization (67). Our candidate-based RNAi screening identified SUN-1, suggesting that SUN-1 may play key roles in recruiting UAD-2 and the USTC complex or heterochromatin to the inner nuclear membrane to create the proper chromatin environment for piRNA transcription.

Materials and Methods

Strains. Bristol strain N2 was used as the standard wild-type strain. All strains were grown at 20 °C unless specified. For the heat stress treatment, worms were cultured at 25 °C for two generations. The strains used in this study were listed in *SI Appendix*, Table S3.

Construction of Plasmids and Transgenic Strains. For the in situ transgene expressing *uad-2::gfp::3xflag*, a UAD-2 promoter and coding sequence (CDS) region were PCR-amplified with the primers 5′- GGGTAACGCCAGCACGTGTGAAGTCTACCTGCCTCCATTG -3′ and 5′- ATAGCTCCACCTCCACCTCCTCCCAGAAGTTTTGAAGACAGTG -3′ from N2 genomic DNA. A GFP::3xFLAG region was PCR-amplified with the primers 5′- GGAGGTGGAGGTGGAGCTATGAGTAAAGG -3′ and 5′- CTTGTCATCGTCATCCTTGTAATCG -3′ from SHG326 genomic DNA. A UAD-2 3′ untranslated region (UTR) was PCR-amplified with the primers 5′- ACA AGGATGACGATGACAAGTAGCTTTTAAAAAATGATTTTTTTTTCATTCGTTTTCTG -3′ and 5′- CCAGCGGATAACAATTTCACAATGCCATGATGGAACAGTCC -3′ from N2 genomic DNA. The coding sequence of GFP::3xFLAG was inserted before the stop codon using the CRISPR-Cas9 system. ClonExpress MultiS One Step Cloning Kit (Vazyme C113-02, Nanjing) was used to connect these fragments with vector which is amplified with 5′-TGTGAAATTGTTATCCGCTGG -3′ and 5′- CACACGTGCTGGCGTTACC -3′ from L4440. The injection mix contained PDD162 (50 ng/ul), UAD-2 repair plasmid (50 ng/ul), pCFJ90 (5 ng/ul), and two sgRNAs (30 ng/ul). The mix was injected into young adult N2 animals. The transgenes were integrated onto the *C. elegans*' chromosome I by CRISPR/Cas9 system.

Construction of Deletion Mutants. For gene deletions, triple-sgRNA–guided chromosome deletion was conducted as previously described (23). To construct sgRNA expression vectors, the 20 bp *unc-119* sgRNA guide sequence in

the pU6::unc-119 sgRNA(F+E) vector was replaced with different sgRNA guide sequences. Addgene plasmid #47549 was used to express Cas9 II protein. Plasmid mixtures containing 30 ng/μl of each of the three or four sgRNA expression vectors, 50 ng/μl Cas9 II expressing plasmid, and 5 ng/μl pCFJ90 were coinjected into *tofu-5::gfp::3xflag* (*ustIS026*) animals. Deletion mutants were screened by PCR amplification and confirmed by sequencing. The sgRNA sequences are listed in *SI Appendix*, Table S4.

Candidate-Based RNAi Screening. RNAi experiments were performed at 20 °C by placing synchronized embryos on feeding plates as previously described (68). HT115 bacteria expressing the empty vector L4440 (a gift from A. Fire) were used as controls. Bacterial clones expressing double-stranded RNAs (dsRNAs) were obtained from the Ahringer RNAi library and were sequenced to verify their identity. All feeding RNAi experiments were performed for two generations except for sterile worms, which were RNAi treated for one generation. Images were collected using a Leica DM4 B microscope.

ChIP. ChIP experiments were performed as previously described with young adults (69). Worm samples of young adult stage were crosslinked in 2% formaldehyde for 30 min. Fixation was quenched with 0.125 M glycine for 5 min at room temperature. Samples were sonicated for 20 cycles (30 s on and 30 s off per cycle) at medium output with a Bioruptor 200. Lysates were precleared and immunoprecipitated with 1.5 μL of rabbit anti-GFP antibody (Abcam, ab290) for TOFU-5 and TOFU-4 overnight at 4 °C. Chromatin/antibody complexes were recovered with Dynabeads Protein A (Invitrogen, 10002D) and followed by extensive sequential washes with 150, 500, and 1 M NaCl. Crosslinks were reversed overnight at 65 °C. Input DNA was treated with RNase (Roche) for 30 min at 65 °C, and all DNA samples were purified using a QIAquick PCR purification kit (Qiagen, 28104).

ChIP-qPCR was performed using a MyIQ2 real-time PCR system with SYBR GREEN mix (Vazyme C112-01, Nanjing). The enrichment of immunoprecipitation was calculated relative to input samples. Intergenic or *ama-1* DNA region was used as controls for sample normalization. The primer sequences are listed in *SI Appendix*, Table S2.

ChIP-Seq. The DNA samples from ChIP experiments were sent to Novogene Bioinformatics Technology Co., Ltd for library preparation and sequencing using an Illumina platform. Briefly, 10 to 300 ng of ChIP DNA was combined with End Repair Mix and incubated for 30 min at 20 °C followed by purification with a QIAquick PCR purification kit (Qiagen). The DNA was then incubated with A-tailing mix for 30 min at 37 °C. The 3′-end adenylated DNA was incubated with the adapter in the ligation mix for 15 min at 20 °C. The adapter-ligated DNA was amplified by several rounds of PCR amplification and purified using a 2% agarose gel to recover the target fragments. The average length was analyzed on the Agilent 2100 bioanalyzer instrument (Agilent DNA 1000 Reagents). The library was quantified by qPCR (TaqMan probe). The libraries were further amplified on cBot to generate the clusters on the flow cell and sequenced with a single-end 50 method on a HiSeq1500 system.

ChIP-Seq Data Analysis and Visualization. ChIP-seq reads were aligned to the ce10 assembly of the *C. elegans* genome using Bowtie 2 version 2.3.5.1 by Ben Langmead with default settings. The samtools version 0.1.19 "view" utility was used to convert the alignments to Binary Alignment Map (BAM) format and "sort" utility was used to sort the alignment files. ChIP-seq peaks were called using MACS2 version 2.1.1 (70) with a permissive 0.01 q-value cutoff against summed ChIP-seq input and run "bdgcmp" utility to generate logLR track. Peaks overlapping blacklisted regions were discarded. Custom Shell scripts were used to convert Bedgraph to Bigwig format. Finally, the Integrative Genomics Viewer genome browser (71) was applied to visualize signals genome-wide and on piRNA clusters.

The deeptools 3.4.3 (72) was used to visualize ChIP-seq profiles over all piRNA genes as heat maps. The "computeGCBias" and "correctGCBias" utility were used to eliminate guanine-cytosine (GC) bias in deep sequencing. Considering the specific enrichment effect of ChIP-seq, 99 bp on both sides of the peak value from MACS2 was excluded in this process. The "bamCoverage" utility and "computeMatrix" utility were used to convert BAM to Bigwig format and taking 1,500 bp of the data group from both side of all piRNA transcription start sites Finally, heat map drawing was performed by the "plotHeatmap" utility.

Recombinant Protein Expression and Purification. The UAD-2 chromodomain (amino acids 57 to 124) and CEC-4 CD domain (amino acids 25 to 141) were PCR-amplified, cloned into plasmid (pET-28a-N8×H-MBP-3C vector), and expressed in the *Escherichia coli* BL21-GOLD (DE3) cells (Novagen). The recombinant proteins were affinity purified through the MBP tag binding to amylose resin (BioLabs) according to manufacturer's instructions.

Histone Peptide Pull-Down Assay. C-terminally biotinylated peptides of *C. elegans* histone H3 (amino acids 1 to 21 and amino acids 14 to 34, unmodified or with trimethylated lysine) were chemically synthesized (SciLight Biotechnology) and used for pull-down assay. The peptides were coupled to High-Capacity Streptavidin Agarose Resin (Thermo Fisher Scientific). Purified MBP fusion proteins (200 μg) were incubated with the peptide-beads slurry in binding buffer (25 mM Tris·HCl, pH 7.5, 250 mM NaCl, 5% glycerol, and 0.1% TritonX-100) for 1 h at 4 °C on a rotator. After washing five times with the binding buffer, bound proteins were released from the beads and resolved by SDS-PAGE gel electrophoresis followed by Coomassie blue staining.

RNA Isolation and Sequencing. Synchronized late young adult worms were sonicated in sonication buffer (20 mM Tris·HCl [PH 7.5], 200 mM NaCl, 2.5 mM $MgCl_2$, and 0.5% Nonidet P-40). The eluates were incubated with TRIzol reagent followed by isopropanol precipitation and DNase I digestion (Qiagen). Small RNAs were subjected to small RNA deep sequencing using an Illumina platform (Novogene Bioinformatics Technology Co., Ltd). Briefly, small RNAs ranging from 18 to 30 nt were gel-purified and ligated to a 3′ adaptor (5′-pUCGUAUGCCGUCUUCUGCUUGidT-3′; p, phosphate; idT, inverted deoxythymidine) and a 5′ adaptor (5′-GUUCAGAGUUCUACAGUCCGACGAUC-3′). The ligation products were gel-purified, reverse transcribed, and amplified using Illumina's small RNA (sRNA) primer set (5′-CAAGCAGAAGACGGCATACGA-3′; 5′-AATGATACGGCGACCACCGA-3′). The samples were then sequenced using an Illumina Hiseq platform.

RNA-Seq Analysis. The Illumina-generated raw reads were first filtered to remove adaptors, low-quality tags, and contaminants to obtain clean reads at Novogene. For mature piRNA analysis, clean reads ranging from 17 to 35 nt were respectively mapped to mature piRNA regions, pre-piRNA regions, and the *C. elegans* transcriptome assembly WS243 using Bowtie2 with default parameters. The number of reads targeting each transcript was counted using custom Perl scripts. The number of total reads mapped to the transcriptome minus the number of total reads corresponding to sense ribosomal RNA (rRNA) transcripts (5S, 5.8S, 18S, and 26S), and sense protein coding mRNA reads were used as the normalization number to exclude the possible degradation fragments of sense rRNAs and mRNAs.

piRNA Gene Annotations. piRNA annotations were downloaded from the piRBase online database (http://www.regulatoryrna.org/database/piRNA). Genomic coordinates of piRNA genes were obtained by SAMtools against the *C. elegans* ce10 genome assembly. Type II piRNA genes were obtained from a previous publication (20). Type I piRNA gene lists were created by filtering the piRBase annotations with type II piRNA genes.

Brood Size. L4 hermaphrodites were singled onto plates and transferred daily as adults until embryo production ceased and the progeny numbers were scored.

Western Blot. Proteins were resolved by SDS-PAGE on gradient gels (10% separation gel, 5% spacer gel) and transferred to a Hybond-ECL membrane. After washing with 1x tris-buffered saline with tween-20 (TBST) buffer (Sangon Biotech, Shanghai) and blocking with 5% milk-TBST, the membrane was incubated for overnight at 4 °C with antibodies. The membrane was washed thrice for 10 min each with 1x TBST and then incubated with secondary antibodies at room temperature for 2 h. The membrane was washed thrice for 10 min with 1x TBST and then visualized. The antibody dilution for the Western blots were as follows: rabbit anti-GFP antibody (Abcam, ab290), 1:5,000; rabbit β-actin (Beyotime, AF5003), 1:4,000.

Statistics. Bar graphs with error bars are presented with mean and SD. All of the experiments were conducted with independent *C. elegans* animals for the indicated N times. Statistical analysis was performed with two-tailed Student's *t* test.

Data Availability. All raw and normalized high throughput sequencing data have been deposited to the China National Center for Bioinformation-National Genomics Data Center under submission number CRA004102.

ACKNOWLEDGMENTS. We are grateful to the members of the S.G. laboratory for their comments. We are grateful to the International *C. elegans* Gene Knockout Consortium and the National Bioresource Project for providing the strains. Some strains were provided by the Caenorhabditis Genetics Center (CGC), which is funded by the NIH Office of Research Infrastructure Programs (Grant P40 OD010440). This work was supported by grants from the National Key Research and Development Program of China (Grants

2018YFC1004500, 2019YFA0802600, and 2017YFA0102900), the Strategic Priority Research Program of the Chinese Academy of Sciences (Grant XDB39010000), the National Natural Science Foundation of China (Grants 91940303, 31870812, 32070619, 31871300, and 31900434), the China Postdoctoral Science Foundation (Grant 2018M632542), the Anhui Natural Science Foundation (Grants 1808085QC82 and 1908085QC96), and the Chinese Academy of Sciences Interdisciplinary Innovation Team. This study was supported, in part, by the Fundamental Research Funds for the Central Universities.

1. N. V. Fedoroff, Presidential address. Transposable elements, epigenetics, and genome evolution. *Science* **338**, 758–767 (2012).
2. M. C. Siomi, K. Sato, D. Pezic, A. A. Aravin, PIWI-interacting small RNAs: The vanguard of genome defence. *Nat. Rev. Mol. Cell Biol.* **12**, 246–258 (2011).
3. M. P. Bagijn *et al*., Function, targets, and evolution of *Caenorhabditis elegans* piRNAs. *Science* **337**, 574–578 (2012).
4. H. C. Lee *et al*., *C. elegans* piRNAs mediate the genome-wide surveillance of germline transcripts. *Cell* **150**, 78–87 (2012).
5. P. W. Reddien, N. J. Oviedo, J. R. Jennings, J. C. Jenkin, A. Sánchez Alvarado, SMEDWI-2 is a PIWI-like protein that regulates planarian stem cells. *Science* **310**, 1327–1330 (2005).
6. D. Palakodeti, M. Smielewska, Y. C. Lu, G. W. Yeo, B. R. Graveley, The PIWI proteins SMEDWI-2 and SMEDWI-3 are required for stem cell function and piRNA expression in planarians. *RNA* **14**, 1174–1186 (2008).
7. E. Schnettler *et al*., Knockdown of piRNA pathway proteins results in enhanced Semliki Forest virus production in mosquito cells. *J. Gen. Virol.* **94**, 1680–1689 (2013).
8. S. Zhao *et al*., piRNA-triggered MIWI ubiquitination and removal by APC/C in late spermatogenesis. *Dev. Cell* **24**, 13–25 (2013).
9. T. Kiuchi *et al*., A single female-specific piRNA is the primary determiner of sex in the silkworm. *Nature* **509**, 633–636 (2014).
10. Z. J. Whitfield *et al*., The diversity, structure, and function of heritable adaptive immunity sequences in the *Aedes aegypti* genome. *Curr. Biol.* **27**, 3511–3519 (2017).
11. S. Kuramochi-Miyagawa *et al*., Mili, a mammalian member of piwi family gene, is essential for spermatogenesis. *Development* **131**, 839–849 (2004).
12. M. A. Carmell *et al*., MIWI2 is essential for spermatogenesis and repression of transposons in the mouse male germline. *Dev. Cell* **12**, 503–514 (2007).
13. M. Reuter *et al*., Miwi catalysis is required for piRNA amplification-independent LINE1 transposon silencing. *Nature* **480**, 264–267 (2011).
14. P. Rangan *et al*., piRNA production requires heterochromatin formation in *Drosophila*. *Curr. Biol.* **21**, 1373–1379 (2011).
15. B. Czech, G. J. Hannon, One loop to rule them all: The ping-pong cycle and piRNA-guided silencing. *Trends Biochem. Sci.* **41**, 324–337 (2016).
16. C. Klattenhoff *et al*., The *Drosophila* HP1 homolog Rhino is required for transposon silencing and piRNA production by dual-strand clusters. *Cell* **138**, 1137–1149 (2009).
17. F. Mohn, G. Sienski, D. Handler, J. Brennecke, The rhino-deadlock-cutoff complex licenses noncanonical transcription of dual-strand piRNA clusters in *Drosophila*. *Cell* **157**, 1364–1379 (2014).
18. P. J. Batista *et al*., PRG-1 and 21U-RNAs interact to form the piRNA complex required for fertility in *C. elegans*. *Mol. Cell* **31**, 67–78 (2008).
19. P. P. Das *et al*., Piwi and piRNAs act upstream of an endogenous siRNA pathway to suppress Tc3 transposon mobility in the *Caenorhabditis elegans* germline. *Mol. Cell* **31**, 79–90 (2008).
20. W. Gu *et al*., CapSeq and CIP-TAP identify Pol II start sites and reveal capped small RNAs as *C. elegans* piRNA precursors. *Cell* **151**, 1488–1500 (2012).
21. G. Cecere, G. X. Y. Zheng, A. R. Mansisidor, K. E. Klymko, A. Grishok, Promoters recognized by forkhead proteins exist for individual 21U-RNAs. *Mol. Cell* **47**, 734–745 (2012).
22. W. S. S. Goh *et al*., A genome-wide RNAi screen identifies factors required for distinct stages of *C. elegans* piRNA biogenesis. *Genes Dev.* **28**, 797–807 (2014).
23. E. M. Weick *et al*., PRDE-1 is a nuclear factor essential for the biogenesis of Ruby motif-dependent piRNAs in *C. elegans*. *Genes Dev.* **28**, 783–796 (2014).
24. R. J. Cordeiro Rodrigues *et al*., PETISCO is a novel protein complex required for 21U RNA biogenesis and embryonic viability. *Genes Dev.* **33**, 857–870 (2019).
25. C. M. Zeng *et al*., Functional proteomics identifies a PICS complex required for piRNA maturation and chromosome segregation. *Cell Rep.* **27**, 3561–3572 (2019).
26. W. Tang, S. Tu, H. C. Lee, Z. Weng, C. C. Mello, The RNase PARN-1 trims piRNA 3′ ends to promote transcriptome surveillance in *C. elegans*. *Cell* **164**, 974–984 (2016).
27. L. M. Kamminga *et al*., Hen1 is required for oocyte development and piRNA stability in zebrafish. *EMBO J.* **29**, 3688 (2010). Correction in: *EMBO J.* **31**, 248 (2012).
28. T. A. Montgomery *et al*., PIWI associated siRNAs and piRNAs specifically require the *Caenorhabditis elegans* HEN1 ortholog henn-1. *PLoS Genet.* **8**, e1002616 (2012).
29. C. Zhang *et al*., mut-16 and other mutator class genes modulate 22G and 26G siRNA pathways in *Caenorhabditis elegans*. *Proc. Natl. Acad. Sci. U.S.A.* **108**, 1201–1208 (2011).
30. K. M. Suen *et al*., DEPS-1 is required for piRNA-dependent silencing and PIWI condensate organisation in *Caenorhabditis elegans*. *Nat. Commun.* **11**, 4242 (2020).
31. A. Ashe *et al*., piRNAs can trigger a multigenerational epigenetic memory in the germline of *C. elegans*. *Cell* **150**, 88–99 (2012).
32. M. Shirayama *et al*., piRNAs initiate an epigenetic memory of nonself RNA in the *C. elegans* germline. *Cell* **150**, 65–77 (2012).
33. H. Mao *et al*., The Nrde pathway mediates small-RNA-directed histone H3 lysine 27 trimethylation in *Caenorhabditis elegans*. *Curr. Biol.* **25**, 2398–2403 (2015).
34. J. G. Ruby *et al*., Large-scale sequencing reveals 21U-RNAs and additional microRNAs and endogenous siRNAs in *C. elegans*. *Cell* **127**, 1193–1207 (2006).
35. A. C. Billi *et al*., A conserved upstream motif orchestrates autonomous, germline-enriched expression of *Caenorhabditis elegans* piRNAs. *PLoS Genet.* **9**, e1003392 (2013).
36. C. Weng *et al*., The USTC co-opts an ancient machinery to drive piRNA transcription in *C. elegans*. *Genes Dev.* **33**, 90–102 (2019).
37. K. A. Senti, J. Brennecke, The piRNA pathway: A fly's perspective on the guardian of the genome. *Trends Genet.* **26**, 499–509 (2010).
38. T. Beltran *et al*., Comparative epigenomics reveals that RNA polymerase II pausing and chromatin domain organization control nematode piRNA biogenesis. *Dev. Cell* **48**, 793–810 (2019).
39. K. B. Beer *et al*., Degron-tagged reporters probe membrane topology and enable the specific labelling of membrane-wrapped structures. *Nat. Commun.* **10**, 3490 (2019).
40. M. V. Almeida, M. A. Andrade-Navarro, R. F. Ketting, Function and evolution of nematode RNAi pathways. *Noncoding RNA* **5**, 8 (2019).
41. A. DasGupta, T. L. Lee, C. Li, A. L. Saltzman, Emerging roles for chromo domain proteins in genome organization and cell fate in *C. elegans*. *Front. Cell Dev. Biol.* **8**, 590195 (2020).
42. S. Jeong, SR proteins: Binders, regulators, and connectors of RNA. *Mol. Cells* **40**, 1–9 (2017).
43. A. Gonzalez-Sandoval *et al*., Perinuclear anchoring of H3K9-methylated chromatin stabilizes induced cell fate in *C. elegans* embryos. *Cell* **163**, 1333–1347 (2015).
44. D. S. Cabianca *et al*., Active chromatin marks drive spatial sequestration of heterochromatin in *C. elegans* nuclei. *Nature* **569**, 734–739 (2019).
45. P. R. Andersen, L. Tirian, M. Vunjak, J. Brennecke, A heterochromatin-dependent transcription machinery drives piRNA expression. *Nature* **549**, 54–59 (2017).
46. J. Ahringer, S. M. Gasser, Repressive chromatin in *Caenorhabditis elegans*: Establishment, composition, and function. *Genetics* **208**, 491–511 (2018).
47. M. Ninova, K. Fejes Tóth, A. A. Aravin, The control of gene expression and cell identity by H3K9 trimethylation. *Development* **146**, dev181180 (2019).
48. B. D. Towbin *et al*., Step-wise methylation of histone H3K9 positions heterochromatin at the nuclear periphery. *Cell* **150**, 934–947 (2012).
49. L. Yan, H. Wu, X. Li, N. Gao, Z. Chen, Structures of the ISWI-nucleosome complex reveal a conserved mechanism of chromatin remodeling. *Nat. Struct. Mol. Biol.* **26**, 258–266 (2019).
50. L. N. Petrella *et al*., synMuv B proteins antagonize germline fate in the intestine and ensure *C. elegans* survival. *Development* **138**, 1069–1079 (2011).
51. O. Matilainen, M. S. B. Sleiman, P. M. Quiros, S. M. D. A. Garcia, J. Auwerx, The chromatin remodeling factor ISW-1 integrates organismal responses against nuclear and mitochondrial stress. *Nat. Commun.* **8**, 1818 (2017).
52. T. Belicard, P. Jareosettasin, P. Sarkies, The piRNA pathway responds to environmental signals to establish intergenerational adaptation to stress. *BMC Biol.* **16**, 103 (2018).
53. B. Yu *et al*., Structural insights into Rhino-Deadlock complex for germline piRNA cluster specification. *EMBO Rep.* **19**, e45418 (2018).
54. D. M. Kasper, G. Wang, K. E. Gardner, T. G. Johnstone, V. Reinke, The *C. elegans* SNAPc component SNPC-4 coats piRNA domains and is globally required for piRNA abundance. *Dev. Cell* **31**, 145–158 (2014).
55. L. B. Bender *et al*., MES-4: An autosome-associated histone methyltransferase that participates in silencing the X chromosomes in the *C. elegans* germ line. *Development* **133**, 3907–3917 (2006).
56. H. Furuhashi, W. G. Kelly, The epigenetics of germ-line immortality: Lessons from an elegant model system. *Dev. Growth Differ.* **52**, 527–532 (2010).
57. E. C. Andersen, H. R. Horvitz, C. Two, Two *C. elegans* histone methyltransferases repress lin-3 EGF transcription to inhibit vulval development. *Development* **134**, 2991–2999 (2007).
58. A. Rechtsteiner *et al*., The histone H3K36 methyltransferase MES-4 acts epigenetically to transmit the memory of germline gene expression to progeny. *PLoS Genet.* **6**, e1001091 (2010).
59. F. W. Schmitges *et al*., Histone methylation by PRC2 is inhibited by active chromatin marks. *Mol. Cell* **42**, 330–341 (2011).
60. W. Yuan *et al*., H3K36 methylation antagonizes PRC2-mediated H3K27 methylation. *J. Biol. Chem.* **286**, 7983–7989 (2011).
61. L. J. Gaydos, A. Rechtsteiner, T. A. Egelhofer, C. R. Carroll, S. Strome, Antagonism between MES-4 and Polycomb repressive complex 2 promotes appropriate gene expression in *C. elegans* germ cells. *Cell Rep.* **2**, 1169–1177 (2012).
62. T. Takasaki *et al*., MRG-1, an autosome-associated protein, silences X-linked genes and protects germline immortality in *Caenorhabditis elegans*. *Development* **134**, 757–767 (2007).
63. M. Smolle *et al*., Chromatin remodelers Isw1 and Chd1 maintain chromatin structure during transcription by preventing histone exchange. *Nat. Struct. Mol. Biol.* **19**, 884–892 (2012).
64. A. Morillon, N. Karabetsou, A. Nair, J. Mellor, Dynamic lysine methylation on histone H3 defines the regulatory phase of gene transcription. *Mol. Cell* **18**, 723–734 (2005).
65. L. A. Boyer, R. R. Latek, C. L. Peterson, The SANT domain: A unique histone-tail-binding module? *Nat. Rev. Mol. Cell Biol.* **5**, 158–163 (2004).
66. C. Lieleg *et al*., Nucleosome spacing generated by ISWI and CHD1 remodelers is constant regardless of nucleosome density. *Mol. Cell. Biol.* **35**, 1588–1605 (2015).
67. A. Daryabeigi *et al*., Nuclear envelope retention of LINC complexes is promoted by SUN-1 oligomerization in the *Caenorhabditis elegans* germ line. *Genetics* **203**, 733–748 (2016).
68. L. Timmons, D. L. Court, A. Fire, Ingestion of bacterially expressed dsRNAs can produce specific and potent genetic interference in *Caenorhabditis elegans*. *Gene* **263**, 103–112 (2001).
69. S. Guang *et al*., Small regulatory RNAs inhibit RNA polymerase II during the elongation phase of transcription. *Nature* **465**, 1097–1101 (2010).
70. J. Feng, T. Liu, B. Qin, Y. Zhang, X. S. Liu, Identifying ChIP-seq enrichment using MACS. *Nat. Protoc.* **7**, 1728–1740 (2012).
71. J. T. Robinson *et al*., Integrative genomics viewer. *Nat. Biotechnol.* **29**, 24–26 (2011).
72. F. Ramírez, F. Dündar, S. Diehl, B. A. Grüning, T. Manke, deepTools: a flexible platform for exploring deep-sequencing data. *Nucleic. Acids Res.* **42**, W187–W191 (2014).